Biochimica et Biophysica Acta 1842 (2014) 2448–2456

Downregulation of G protein-coupled receptor kinase 2 levels enhances cardiac insulin sensitivity and switches on cardioprotective gene expression patterns

Elisa Lucas[1,2,&], María Jurado-Pueyo[1,2,&], María A. Fortuño[3], Sonia Fernández-Veledo[4], Rocío Vila-Bedmar[1,2], Luis J. Jiménez-Borreguero[2,5], Juan J. Lazcano[5], Ehre Gao[6], Javier Gómez-Ambrosi[7], Gema Frühbeck[7], Walter J. Koch[6], Javier Díez[3,8], Federico Mayor Jr.[1,2,*] and Cristina Murga[1,2,*].

[1] Departamento de Biología Molecular and Centro de Biología Molecular Severo Ochoa (UAM-CSIC), Madrid, Spain.

[2] Instituto de Investigación Sanitaria La Princesa, Madrid, Spain.

[3] Division of Cardiovascular Sciences, Centre for Applied Medical Research (CIMA), University of Navarra, Pamplona, Spain.

[4] Hospital Universitari de Tarragona Joan XXIII, IISPV, Universitat Rovira i Virgili, CIBERDEM Spain.

[5] Centro Nacional de Investigaciones Cardiovasculares (CNIC), Madrid, Spain

[6] Department of Pharmacology and Center for Translational Medicine, Temple University, Philadelphia, USA.

[7] Metabolic Research Laboratory, Universidad de Navarra, CIBERobn,Pamplona, Spain.

[8] Department of Cardiology and Cardiovascular Surgery, University Clinic, University of Navarra, Pamplona, Spain.

[&]equal contribution to this work

[*] corresponding authors

Contact information:

Centro de Biología Molecular Severo Ochoa

c/Nicolás Cabrera, 1

Universidad Autónoma, 28049 Madrid, Spain

cmurga@cbm.uam.es; Phone: 34-91-1964641; Fax: 34-91-196-4420

fmayor@cbm.uam.es ; Phone: 34-91-1964626; Fax: 34-91-196-4420

Abbreviations: GPCR, G protein-coupled receptor; GRK2, G protein-coupled receptor kinase 2; IR, insulin resistance; HF, heart failure; HFD, High fat diet; WT, wild type.

ABSTRACT

G protein-coupled receptor kinase 2 (GRK2) has recently emerged as a negative modulator of insulin signalling. GRK2 downregulation improves insulin sensitivity and prevents systemic insulin resistance (IR). Cardiac GRK2 levels are increased in human heart failure, while genetically inhibiting GRK2 leads to cardioprotection in mice. However, the molecular basis underlying the deleterious effects of GRK2 up-regulation and the beneficial effects of its inhibition in the heart are not fully understood. Therefore, we have explored the interconnections among a systemic IR status, GRK2 dosage and cardiac insulin sensitivity in adult (9 month-old) animals. $GRK2^{+/-}$ mice display enhanced cardiac insulin sensitivity and mild heart hypertrophy with preserved systolic function. Cardiac gene expression is reprogrammed in these animals, with increased expression of genes related to physiological hypertrophy, while the expression of genes related to pathological hypertrophy or to diabetes/obesity co-morbidities is repressed. Notably, we find that cardiac GRK2 levels increase in situations where IR develops, such as in ob/ob mice or after high fat diet feeding. Our data suggest that GRK2 downregulation/inhibition can help maintain cardiac function in the face of co-morbidities such as IR, diabetes or obesity by sustaining insulin sensitivity and promoting a gene expression reprogramming that confers cardioprotection.

Key words: G protein-coupled receptors; GRK2; insulin resistance; cardiac hypertrophy; heart failure; high fat diet.

1. INTRODUCTION

G protein-coupled receptor kinases (GRKs) were initially identified as serine-threonine kinases able to phosphorylate agonist-activated G protein-coupled receptors (GPCRs), triggering the binding of arrestins to the receptor, what impairs G protein coupling in a process known as desensitization [1]. However, very recent findings suggest that the GRK2 isoform is also a key controller of insulin receptor signaling [2]. GRK2 downregulation can prevent the development of metabolic disorders, modulating energy expenditure and brown fat function [3] and also insulin actions in peripheral tissues [2]. Notably, $GRK2^{+/-}$ mice (expressing 50% less protein than control littermates) show improved systemic insulin sensitivity, display enhanced activation of the insulin-mediated Akt pathway in muscle, adipose tissue and liver, and are resistant to the induction of insulin resistance (IR) in three different mouse models of this condition [2]. Remarkably, such differences in insulin sensitivity between wild type (WT) and GRK2 hemizygous mice were noted in the adult stage but were not evident in young animals [2].

GRK2 has also been described to play a relevant role in cardiovascular physiopathology. Increased cardiac GRK2 levels have been reported in patients with ischemic or idiopathic dilated cardiomyopathy, cardiac ischemia, hypertension, volume overload and left ventricular hypertrophy [1, 4, 5]. Also, enhanced GRK2 expression induced by neurohormonal activation has been associated with lower cardiac function and poorer prognosis in human heart failure (HF) and appears as an early event in maladaptive cardiac remodelling in HF [5-7], altogether putting forward GRK2 as a relevant therapeutic target in this myocardial disease (reviewed in ref. [6]). Consistently, genetic inhibition of GRK2 is cardioprotective in different animal models ([1, 5-8] and references therein), and hemizygous GRK2 mice are hyper-responsive to catecholamines and display enhanced cardiac contractility and function, whereas transgenic mice overexpressing different levels of this kinase show an impaired adrenergic cardiac response [9]). However, the detailed molecular mechanisms and the relevant functional interactions underlying the deleterious effects of elevated GRK2 levels in cardiac function and the beneficial effects of its inhibition remain to be fully established.

In principle, up-regulation of GRK2 in HF would further exacerbate the marked β-adrenergic desensitization observed in such condition. However, chronic adrenergic activation appears to be more detrimental than beneficial for heart disease and, most

importantly, β-blockers represent a successful standard treatment for this disease. In this context, the fact that GRK2 inhibition acts in a synergic manner with established β-blocker treatments (reviewed in [6, 7]) suggests these two therapeutic strategies must have independent mechanisms of action. Thus, the functional impact of altered GRK2 levels might also be related to the interactions of this protein with cellular partners other than β-adrenergic receptors [10].

In this regard, adding to the data showing that GRK2 up-regulation inhibits insulin signaling in muscle or adipose tissue [2], recent findings have suggested that cardiac-specific overexpression of GRK2 inhibits glucose uptake and promotes IR after myocardial ischemia in young mice [11]. However, the potential interconnections among a systemic IR status, GRK2 levels and the cardiac maladaptive remodeling linked to cardiac dysfunction have not been addressed to date.

In this report, we have characterized the activation of insulin signaling pathways, tissue remodeling in the heart and cardioprotective gene expression patterns in young and adult WT and $GRK2^{+/-}$ mice. This experimental model allows us to explore the consequences of a chronic, physiological-range change in GRK2 levels with age (a risk factor for the onset of most cardiovascular pathologies) that would mimic the long sought pharmacological systemic inhibition of GRK2 as a potential drug target. In addition, we have investigated the effect of systemic IR-promoting conditions on cardiac GRK2 levels and its impact on cardiac insulin responses. Our data point at new molecular links between GRK2 up-regulation in IR-related situations and maladaptive cardiac remodeling in the adult mouse heart.

2. MATERIALS AND METHODS

2.1 Animals

Experiments were performed on male wild type and hemizygous-GRK2 ($GRK2^{+/-}$) mice maintained on the hybrid 129/SvJ C57BL/6 background. The animals were bred and housed on a 12-hour light/dark cycle with free access to food and water. $GRK2^{+/-}$ mice, as well as male leptin-deficient obese *ob/ob* mice (C57BL/6J-Lep^{ob}/Lep^{ob}) and their corresponding wild types (C57BL/6J, The Jackson Laboratory, Bar Harbor, ME, USA) were fed *ad libitum* since weaning either on a normal chow diet (providing 13% of total calories as fat, 67% as carbohydrate and 20% as protein; 2014S Rodent Maintenance Diet, Teklad, Harlan, Barcelona, Spain) or a high fat diet (providing 45% of total calories as fat, 35% as carbohydrate and 20% as protein, Rodent Diet D12451, Research Diets, New Brunswick, NJ, USA). Animals were maintained at a room temperature of 22±2 ºC on a 12:12 light-dark cycle (lights on at 08:00 am) with a relative humidity of 50±10% and under pathogen-free conditions. All animal experimentation procedures conformed to the European Guidelines for the Care and Use of Laboratory Animals (Directive 86/609) and approved by the Ethical Committees for Animal Experimentation of the Universidad Autonoma de Madrid and the University of Navarra (protocols 013/08 and 041/08).

2.2 Plasma membrane preparation and GLUT4 translocation quantification

Relative quantification of GLUT4 protein in the plasma membrane fraction was achieved by a subcellular fractionation method modified from Rett K. et al [12]. Mice were injected intravenously in the tail vein with insulin (1 unit/kg of body weight). After 25 minutes, mice were sacrificed by cervical dislocation and hearts were homogenized using metal beads in a Tissue Lyser using cooled buffer (200 mM Tris-HCl pH 7.5, 10mM EDTA, 255 mM Sucrose) with protease inhibitors (100 µM PMSF, 1 µM benzamidine, 10 µg/ml STI, 16 µU aprotinin, 10 µg/ml bacitracin). Lysates were centrifuged at 9000 x g for 20 minutes. The pellet (P1) was resuspended in buffer, homogenized again and centrifuged at 200 x g for 20 minutes. The plasma membrane-enriched P2 was then resuspended and homogenized in RIPA buffer (100 mM Tris-HCl pH 7.4, 600 mM NaCl, 2% Triton X-100, 0.2% sodium dodecyl sulfate, 1% deoxycholate plus protease inhibitors) for Western Blot analysis. Protein content was quantified using the Lowry procedure and 40 µg of total protein were resolved on a 12% SDS-PAGE gel and transferred to a nitrocellulose membrane. Blots shown here were probed with specific antibodies against GLUT4 (EMD Millipore, Darmstadt, Germany), Caveolin 3 (BD Transduction Laboratories, Franklin Lakes, NJ, USA) and α-Tubulin (Santa Cruz Biotechnology, Dallas, TX, USA).

2.3 Insulin treatments and Western Blots

Insulin (Actrapid®, Novo Nordisk, Bagsvaerd, Denmark) solution in saline serum (1unit/kg body weight) was administered by tail vein injection for acute cardiac insulin pathway activation analysis. After either 3 or 5 minutes, mice were sacrificed by cervical dislocation and hearts were quickly collected, washed and frozen at -70 ºC. Heart tissue was homogenized using metal beads in a Tissue Lyser using hypotonic buffer (20 mM Tris-HCl pH 7.5, 1 mM EDTA, 1 mM EGTA) completed with protease and phosphatase inhibitors (100 µM PMSF, 1 µM benzamidine, 10 µg/ml STI, 16 µU aprotinin, 10 µg/ml bacitracin and Phosphatase Inhibitor Cocktail -PhosSTOP, (Roche, Indianapolis, IN, USA)- following manufacturer´s protocol). Then 0.1% (v/v) Triton X-100 was added and the samples were agitated for 1 h. at 4ºC, and centrifuged to measure supernatants protein content using the Lowry procedure. For Western Blot analysis, typically 40 µg of total cardiac protein was resolved per lane on a 7.5% SDS-PAGE gel and transferred to a nitrocellulose membrane. Blots were probed with specific antibodies against phospho-Akt (Ser473), Akt, phospho-p70S6K (Thr389), phospho-ERK1/2 (Thr202/Tyr204) (Cell SignallingTechnology, Beverly Ma, USA), p70S6K, phospho-IRS1 (Tyr896) (BD

biosciences,Franklin Lakes, NJ, USA), ERK-1, ERK-2, GRK2, Nucleolin (Santa Cruz Biotechnology, Dallas, TX, USA) ,GAPDH (Abcam,Cambridge, UK) and IRS1-PH (kindly provided by Deborah J. Burks, Spain) [13].

2.4 Cardiac morphometry

For the histological and morphometric analysis of the hearts, mice were anesthetized with isoflurane and an intracardiac injection of cold KCl solution was used to stop the heart in diastole before the heart collection. Hearts were weighted for cardiac index determination, and the medial section was fixed in formaldehyde and embedded in paraffin prior to transversal sectioning using a microtome. Masson´s Trichrome staining was performed for the morphometric analysis and Syrius red staining for fibrosis quantification. Images were analyzed using the AnalySIS® software (Soft Imaging System).

2.5 Echocardiography

To measure global systolic cardiac function and left ventricular mass (LVM), echocardiography was performed in 9 month-old WT and hemizygous GRK2 mice. Mice were anaesthetized by inhalation of isoflurane/oxygen (1.25%/98.75%) and examined by a 30 MHz transthoracic echocardiography probe. Images were obtained with Vevo 770 (VisualSonics, Toronto, Canada). The internal diameter of the LV was measured in the short-axis view from M-mode recordings in end diastole and end systole and ejection fraction (EF) and fractional shortening (FS) were calculated using the formulas as previously described [14].

2.6 RNA isolation and microarray analysis

mRNA from frozen heart tissue was extracted using metal beads (2 min, 30 Hz) in a Tissue Lyser and Fibrous Tissue RNeasy Mini Kit, both from QIAGEN (Hilden, Germany). Three mice per condition were used for the gene expression profile analysis of $GRK2^{+/-}$ and WT mice of 4 and 9 months of age. cDNA synthesis, labeling and microarray analysis were performed with the aid of the Bioinformatics group at the National Center of Biotechnology (CNB, Madrid, Spain). Generation of double-stranded cDNA, preparation and labelling of cRNA, hybridization to GeneChip® Mouse Genome 430 2.0 Arrays (Affymetrix, Santa Clara, CA, USA) and washing was performed according to the protocol provided by Affymetrix. Probe sets were summarized using the LiMMA algorithm. Results were analyzed and visualized using Researcher´s Digest software and FIESTA viewer respectively, as well as Multiexperiment Viewer software (TM4 Microarray Software Suite).

2.7 Co-immunoprecipitation assays

Cell lysates obtained as previously described for Western Blot were quantified using the Lowry procedure. Next, 500 µg total protein per lysate were incubated with 10 µl of either rabbit IgG or IRS1 antibody (Santa Cruz Biotechnology, Dallas, TX, USA) and 0.4 µg/µl BSA on a rotating shaker at 4°C overnight and 15 µl of Protein G-Sepharose (50% in lysis buffer) were added to each tube. After 2 hours on a rotating shaker at 4°C, tubes were centrifuged at 14000 x g for 5 seconds and the pellets were washed with pre-chilled washing buffer (hypotonic-1% Triton) for 10 times (1ml each). Pellets were then boiled in 4x Laemmli loading buffer for 5 minutes and used for Western Blot analysis. Blots were probed with specific antibodies against IRS1-PH [13] and GRK2 (Santa Cruz Biotechnology, Dallas, TX, USA).

2.8 RT-PCR and microarray validation

mRNA from heart tissue of at least 6 WT and 6 GRK2$^{+/-}$ mice was isolated as described before. RT-PCRs were performed by the Genomic Facility at CBMSO using Light Cycler equipment (Roche, Indianapolis, IN, USA). Microarray validations were performed using both commercial Taqman Gene Expression Assay probes (Applied Biosystems,Life Technologies, Grand Island, NY, USA) and self-designed probes purchased from Sigma with Syber Green technology. qPCRs and statistical analysis of the data were performed by the Genomic Facility at CBMSO using GenEx software.

2.9 Small-animal PET protocol

2-deoxy-2-[18F]-fluoro-D-glucose in isotonic saline solution was injected through the intravenous catheter of WT and GRK2+/- adult mice to characterize heart glucose utilization in basal and after 5-min insulin stimulation. 90-minutes dynamic imaging was performed with a piPET scanner and tomographic images were reconstructed using a three-dimensional ordered subset expectation maximization algorithm as previously described [15] . Region of interest measurements were made on multiple axial slices of the myocardium and tracer uptake was quantified as standardized uptake values normalized by injected dose and corrected for body weight.

2.10 Statistics

Data were analyzed by one-way ANOVA, followed by a Bonferroni's *post hoc* analysis, or by unpaired *t*-testing when specified, as appropriate. For all tests, $P < 0.05$ was considered statistically significant after Bonferroni corrections, if needed, and all data are reported as means ± SEM.

3. RESULTS

3.1 Decreased GRK2 levels correlate with enhanced cardiac insulin sensitivity

GRK2 can act as a negative modulator of insulin receptor signalling pathways, and adult GRK2$^{+/-}$ mice show improved systemic insulin sensitivity and are resistant to the induction of IR in peripheral tissues [2]. In this context, we explored the possibility that GRK2 dosage could modify heart insulin sensitivity *in vivo* in 9 month-old mice. The translocation to the plasma membrane of the GLUT4 glucose transporter is a key early event in glucose uptake stimulated by insulin. As can be observed in Figure 1a, insulin-dependent GLUT4 translocation was significantly enhanced in adult GRK2 hemizygous mice, compared to wild-type animals, as assessed by Western Blot analysis of membrane fractions of cardiac tissue. These results are in agreement with the increased accumulation of labelled deoxyglucose in the hearts of GRK2$^{+/-}$ mice quantified by PET (Supplementary Figure 1S). A similar pattern was observed for the rapid stimulation of Akt and its downstream target p70S6K kinase detected with specific phospho-antibodies upon injection of insulin (Fig. 1b-e).

Of note, upstream insulin signalling events such as the amount of phospho-Tyrosine(Tyr896)IRS1 was increased in GRK2$^{+/-}$ hearts after insulin stimulation while the activation status of the ERK cascade was not affected (Supplementary Fig. 1S b-d). Together, these results demonstrate that the metabolic and pro-survival signals downstream of insulin were more potently activated in GRK2$^{+/-}$ hearts than in WT mice.

3.2 GRK2$^{+/-}$ 9 month-old mice display mild, non-pathological heart hypertrophy

The modulation of the PI3K/Akt and the ERK pathways in the heart is shared by insulin, IGF-1 and hypertrophic agonists such as angiotensin II. The PI3K/Akt cascade relates mostly to physiological hypertrophy, whereas MAPK signalling, together with PKC and calcineurin/NFAT, participates in the development of the pathological hypertrophy typically induced by angiotensin II (reviewed in ref. [16]).

We found that GRK2$^{+/-}$ mice showed a modest but significant increase in heart to body weight ratio and in the total cardiac area with age compared to the change observed in WT animals (Fig. 2a and 2b). We also found an enhanced increase in cardiomyocyte diameter in GRK2$^{+/-}$ animals (Fig. 2c), an established indicator of cardiac hypertrophy. No differences in these parameters were found at 4 months of age between WT and GRK2$^{+/-}$ animals. Echocardiographic analysis also revealed a certain degree of hypertrophy in the 9 month-old hemizygous mice, mainly referred to left ventricular mass (data not shown) in the absence of any alterations in cardiac functionality, as defined by fractional ejection (EF) or fractional shortening (FS) parameters (Fig. 2d). Consistently, fibrosis was not increased in either 4 or 9 month-old GRK2$^{+/-}$ mice compared with age-matched controls (Fig. 2e).

3.3 Decreased GRK2 levels correlate with the expression of key genes involved in physiological hypertrophy/cardioprotection

Insulin is known to play a protective role in cardiac physiology, via the control of cardiac substrate utilization, cardiomyocyte growth, gene expression, survival and contractility by means of the homeostatic stimulation of the PI3K/Akt and other intracellular signalling pathways [17] . As an unbiased approach to assess the functional consequences of altering GRK2 levels in the modulation of insulin response and heart function, we compared the transcriptional profile of the cardiac tissue of WT and GRK2$^{+/-}$ mice of 4 or 9 months of age using microarray RNA expression techniques without subjecting the animals to prior specific treatments to study the integrated response of the tissue to homeostatic endogenous signals. Comparison of gene expression profiles between WT and GRK2$^{+/-}$ animals at each group of age (database access number GSE41706) revealed significant differences only at 9 months (33

genes significantly up-regulated and 28 genes down-regulated in GRK2$^{+/-}$ mice compared to WT) while no differences between genotypes were detected at 4 months of age (Figure 3a and Suppl. Table 1), suggesting that the effects of GRK2 dosage on cardiac gene expression require additional age-related changes to become apparent.

We next performed a detailed analysis of the function and characteristics of the up or down-regulated genes. Several interesting patterns were noted. First, GRK2$^{+/-}$ mice at 9 months of age showed decreased expression of genes described to be up-regulated during pathological heart hypertrophy and/or in well-characterized cardiovascular disease co-morbidities such as diabetes and obesity. Eight out of the 28 genes down-regulated in GRK2$^{+/-}$ mice (29%) belonged to this group (see Fig. 3b). This list included the pivotal heart hypertrophy markers *Acta1* (skeletal muscle alpha-actin) and the atrial natriuretic factor precursor *Nppa* [18, 19]; the cardiovascular heat shock protein *Hspb7*, with high expression in ob/ob mice skeletal muscle [20] and polymorphisms associated with development of idiopathic dilated cardiomyopathy and heart failure [21]; the transcription factor promyelocytic zing finger protein (*Plzf*, also known as *Zbtb16*), a mediator of angiotensin 2-type 2 receptor-triggered cardiac hypertrophy [22]; the microfibril-associated glycoprotein-2 (*Magp-2*, also known as *Mfap5*), an angiogenic stimulator upregulated in transgenic models of HF [23], or the tissue inhibitor of metalloproteinase 4 (*Timp4*), a proposed marker for left ventricular remodelling and deteriorating HF [24]. Prostaglandin D synthase (*Ptgds*), increased in the coronary circulation of angina patients [25] and overexpressed in type 2 diabetes [26] and the p85 alpha PI3K regulatory subunit (*Pik3R1*), enhanced in the myocardium of mice developing diet-induced obesity [27] and a key negative regulator of insulin signaling [28, 29] were also decreased in 9 month-old GRK2$^{+/-}$ hearts.

A second interesting pattern found in GRK2$^{+/-}$ mice was that 10 out of 33 genes that were up-regulated in these animals (30%) have been reported to play a protective role in cardiovascular disease and are often down-regulated in pathological heart hypertrophy and/or diabetes/obesity co-morbidities (Fig. 3b). In this regard, the expression of *Ppargc1b, Hdac9*, *RRad*, or *Pde4b*, reported as key negative regulators of pathological heart hypertrophy, was enhanced in GRK2$^{+/-}$ mice. PGC1beta (Peroxisome proliferator-activated receptor (PPAR)-gamma1beta co-activator) is essential for mitochondrial biogenesis and energy homeostasis. Decreased *Ppargc1b* expression correlates with cardiac insufficiency and cardiomyopathy and with obesity and type-2 diabetes, whereas its genetic deletion accelerates the transition to HF following pressure overload hypertrophy [30, 31]. HDAC9 is an inhibitor of pathological (but not physiological) cardiac hypertrophy and *Hdac9*-deficient mice exhibit stress-dependent cardiomegaly [32]. RRAD (Ras associated with diabetes GTPase) levels are decreased in human failing hearts and in animal and cellular models of cardiac hypertrophy, and *RRad*-deficient mice are more susceptible to this condition [33]. RRAD appears to prevent CAMK-II-dependent hypertrophy, to inhibit cardiac fibrosis and to modulate beta-adrenergic mediated contractility [33, 34]. Phosphodiesterase 4B (PDE4B) is an important, protective negative modulator of beta-adrenergic-mediated contractility with decreased levels in cardiac hypertrophy [35]. Thrombospondin 1 (*Thbs1*), a protein that modulates extracellular matrix metabolism and fibroblast phenotype, suggested to act as a protective signal in the stressed heart [36] was also enhanced in GRK2$^{+/-}$ mice, as was the anti-angiogenic homeobox gene *Meox2* [37].

The third relevant pattern of differential expression detected in GRK2$^{+/-}$ mice reflects changes in the expression of genes similar to those taking place upon exercise and in situations of physiological heart hypertrophy (Fig. 3b). These include the up-regulation of the central protective factors *Ppargc1b* and *Nr4a1* (see above); the early response genes *FosB* and *Apold 1*, reported to be enhanced in cardiac tissue upon acute physical activity [38] and the downregulation of the transcription factor C/EBPbeta (*Cebpb)*, a member of the bHLH family. Importantly, the latter has been recently identified as a master regulator of physiological cardiac hypertrophy [39, 40]. The mRNA expression of C/EBPbeta is reduced *circa* 60% (in the same range of our data) in mouse hearts in an exercise model allowing expression of an adaptive gene profile related to physiological hypertrophy, and mice with reduced cardiac levels of this

protein displayed resistance to cardiac failure upon pressure overload [39]. The expression profile of several of the key genes supporting these patterns was validated by qPCR (Suppl. Fig. 2S).

In sum, the microarray analysis detected in GRK2$^{+/-}$ mice hearts an increased expression of a limited group of important genes related to physiological hypertrophy while the expression of genes key to the development of pathological hypertrophy or related to diabetes/obesity co-morbidities is repressed.

3.4 Increased cardiac GRK2 expression in adult obese (ob/ob) mice and in high fat diet-fed animals

Since GRK2 levels increase in muscle and adipose tissue under insulin resistance-promoting conditions [2] we tested whether this process was also taking place in cardiac tissue. A clear increase in GRK2 protein levels was observed in hearts of 8 month-old *ob/ob* mice (Fig. 4a), an age in which this strain of mice is known to manifest cardiac hypertrophy, IR and metabolic alterations involving alterations in the PI3K/Akt axis [41]. This increase in total GRK2 protein levels caused an increment in the amount of GRK2 that could be detected in association with IRS1 (Fig. 4b), a situation that we have previously described to negatively modulate insulin signaling. GRK2 levels were also increased upon feeding young animals a high fat diet (HFD, Fig. 4c), a well-established trigger for systemic IR that can promote cardiac remodeling and dysfunction and known to disrupt the insulin-stimulated IRS1/PI3K/Akt cascade [42]. This increase is similar to that observed in other insulin-sensitive tissues [2], and also had as a consequence a larger amount of formation of IRS1-GRK2 complexes (Fig. 4d). We investigated insulin responses in cardiac tissue of WT and GRK2$^{+/-}$ HFD-fed animals. Figure 4e-f shows that sensitivity to insulin is compromised in WT hearts after HFD feeding, while it is strongly preserved in GRK2$^{+/-}$ hearts, in the absence of changes in insulin-induced ERK phosphorylation. Together these results suggest that the increase in GRK2 protein levels observed upon HFD feeding or genetically-induced obesity promotes GRK2-dependent sequestration of IRS1 and provides a mechanistic explanation for the IR state of cardiac tissue in both experimental conditions.

4. DISCUSSION

We have addressed herein the potential interconnections among an IR status, GRK2 dosage and cardiac remodeling by investigating the impact of GRK2 down-modulation on cardiac insulin sensitivity and gene expression patterns, and the effects of systemic insulin resistance-promoting conditions on cardiac GRK2 levels.

First, we find that decreased GRK2 levels specifically preserve metabolic and pro-survival signals downstream of insulin (such as the Akt/p70S6K pathway and glucose transport) in the hearts of 9 month-old GRK2$^{+/-}$ animals, whereas the ERK activation status is not affected. Second, with age, GRK2 down-regulation triggers physiological heart hypertrophy and switches on a cardioprotective gene expression pattern as detected in such adult mice. This pattern is characterized by an increased expression of a limited group of key genes related to physiological hypertrophy, while the expression of genes reported to lead to the development of pathological hypertrophy or related to diabetes/obesity co-morbidities is repressed, compared to WT individuals. Third, we uncover that cardiac GRK2 expression levels increase in situations of systemic insulin resistance, such as in obese mice or after HFD feeding, conditions in which larger amounts of GRK2-IRS1 complexes are formed. Fourth, while insulin resistance develops in the hearts of wild-type mice after HFD feeding, sensitivity to insulin was strongly preserved in GRK2$^{+/-}$ cardiac tissue.

We have previously reported that GRK2$^{+/-}$ mice are protected against HFD-induced obesity and systemic IR, and we cannot rule out that this global protection may contribute to the observed enhanced insulin signaling in the heart upon a HFD. However, given the enhanced interaction of GRK2 with IRS1 that we find in cardiac tissue of different obese mice models, our data point at an important role for this kinase in negatively regulating insulin signaling in the heart, coherent with what was previously published by Garcia-

Guerra et al. [2] involving the sequestration of IRS1 protein in GRK2 complexes thus impairing downstream signalling from the insulin receptor.

Previous reports have determined the importance of insulin signalling in cardiac physiopathology [43]**.** In particular, results in cardiomyocyte-specific deletion of the insulin receptor (CIRKO mice) have revealed that insulin can control cardiac gene expression patterns since loss of its receptor promotes a genomic reprogramming [44]. Insulin signals also control the size of the heart and cardiomyocytes, and deletion of insulin receptor decreases cardiac size by 20-30% [45]. These results are in agreement with the phenotype we find in GRK2 hemizygous mice in which the increased sensitivity for insulin signals results in gene expression reprogramming and an increased cardiac size.

The fact that GRK2 downregulation potentiates the insulin-triggered PI3K/Akt pathway in the adult mice heart is then consistent with the mild hypertrophic phenotype conferred by age to $GRK2^{+/-}$ animals being physiological rather than pathological, This is in agreement with the morphometric analysis and functional results, and with an overall cardio-protective gene expression pattern (decreased presence of pathological genes, enhanced expression of critical protective genes) in the heart of $GRK2^{+/-}$ 9 month-old mice. It is worth noting that $GRK2^{+/-}$ animals displayed changes in the expression of several genes reported to be similarly modulated by insulin in the heart or other tissues (*Nr4a1*, *Tcfl2*, *Rrad, Aqp7*, *Cebpb*, *Ppargc1b*, *Egr1*), and a relevant proportion of genes whose expression is altered in hemizygous animals can be related to: i) the modulation of insulin sensitivity; ii) to the PI3K/Akt pathway; iii) to diabetes/obesity-related pathological situations.

Insulin activation of the PI3K/Akt cascade is protective in the heart by inhibiting apoptosis and oxidative stress [46], whereas myocardial IR has been suggested as a key factor in the development of HF [47, 48]. In this context, our results strongly suggest the novel concept that cardiac GRK2 levels could act as an integrative sensor of different pathological inputs and affect cardiac function by simultaneously altering beta-adrenergic and insulin signalling (see suggested model in Fig. 5). Thus, the increase in cardiac GRK2 levels previously reported to take place in myocardial infarction or hypertension as a consequence of excessive neurohormonal stimulation [5, 6], would also take place as a consequence of insulin resistance-promoting conditions such as a HFD or obesity, by mechanisms that remain to be investigated. Also, enhanced cardiac GRK2 would promote, in addition to the canonical effects described for GPCR signaling, an insulin-resistant state of the heart leading to alterations of key metabolic and cardioprotective pathways [11], further fuelling a dysfunctional cycle and allowing progression to maladaptive remodelling.

A detrimental vicious cycle has been postulated [48, 49] in which the compensatory hyper-adrenergic state characteristic of reduced cardiac output would promote lipolysis in the adipose tissue. This would lead to increased circulating levels of free fatty acids, what in turn would inhibit cardiac glucose transport, switching energy substrate use and triggering heart lipotoxicity. Conversely, many mechanisms have been suggested to explain the increased incidence of HF in diabetic patients, including hyperinsulinemia, hyperglycemia, lipotoxicity, obesity, vascular alterations, increased oxidative stress or hyperactivation of neurohumoral systems ([47, 48, 50] and references therein). Our data suggest that GRK2 could participate as an important integrative node in such complex mechanisms linking HF, diabetes and IR.

Such central role of GRK2 also fosters its potential as a therapeutic target and diagnostic marker. Our study suggests that strategies leading to a systemic reduction in GRK2 levels/function, even when used in a sustained temporal frame and in adult tissue, could facilitate the activation of defined cardioprotective routes*,* such as the insulin pathway. This would promote a physiological hypertrophy-like gene expression pattern that could contribute to explain the beneficial outcome of GRK2 inhibition.

This discovery could help explain the reported reinforcement between the therapeutic effects of down-regulating cardiac adrenergic input (using beta-blockers) and GRK2 down-modulation.

Since our data and previous report by other laboratories [1, 6, 7] indicate that reduced GRK2 revels are beneficial for cardiac function and also for maintaining vascular tone [4], and systemic insulin sensitivity [2], it could be argued that GRK2 hemizygosity would confer an overall benefit. However, the fact that a $GRK2^{+/+}$ genotype has been positively selected for by evolution suggest that the expression level generated by such genotype must be overall adaptative. Nevertheless, unlimited food availability, a condition that humans nowadays share with caged animals, was not at all present during evolution and therefore this might explain why GRK2 downregulation was not selected for.

GRK2 inhibition has been shown, in mouse models, to delay the reduction in glucose uptake and preserve insulin signalling in the heart after myocardial ischemia [11] and to prevent the development of systemic IR [2]. It is also worth noting that, apart from its catalytic kinase activity (target for potential GRK2 inhibitors), GRK2 plays an important functional role via protein-protein interactions. Our gene expression data cannot dissect which biological function of GRK2 needs to be reduced for therapeutic purposes, and it could well be possible that inhibition of the enzymatic activity of GRK2 might not reproduce the beneficial effects observed upon its under-expression. Thus, a better knowledge of means to reduce GRK2 levels *in vivo*, such as increasing its degradation rate or decreasing transcription, should be built before an effective GRK2 downmodulation therapy can be designed. Interestingly, ventricular assist device implantation, known to downregulate GRK2 levels [51], also reverses IR and normalizes cardiac metabolism in patients with advanced HF[52]. This is consistent with a beneficial role for GRK2 inhibition in this context. Notably, the reduction in GRK2 protein levels observed in lymphocytes of HF patients after an exercise-training program can predict long-term survival [53]. On the other hand, enhanced GRK2 levels in peripheral lymphocytes mimic myocardial levels during hypertension, myocardial ischemia and heart failure [6] and are also increased in patients with metabolic syndrome [2]. Therefore, it will be interesting to explore the potential use of GRK2 as a prognostic cardiovascular risk marker when co-morbidities as diabetes, IR and obesity are present.

5. ACKNOWLEDGEMENTS

We thank Dr. F. Sánchez Madrid (IIS La Princesa and CNIC, Madrid, Spain) for access to their animal facilities, J.J. Vaquero (PET scanning facility, Gregorio Marañon Hospital, Madrid) and Dr. N. López-Andrés and Dr. C. Iñigo (CIMA, Pamplona, Spain) for advice with cardiac morphometry experiments.

Our laboratory is funded by grants from Ministerio de Educación y Ciencia (SAF2011-23800), Fundación para la Investigación Médica Aplicada (FIMA) and UTE project CIMA, The Cardiovascular Network of Ministerio Sanidad y Consumo-Instituto Carlos III (RD06-0014/0037 and RD12/0042/0012), Comunidad de Madrid (S2010/BMD-2332) and EFSD-Novo Nordisk to F.M and UAM-Grupo Santander to C.M and Wood-Whelan Research Fellowship from IUBMB to E.L. We also acknowledge institutional support from Fundación Ramón Areces.

6. REFERENCES

[[1] E.V. Gurevich, J.J. Tesmer, A. Mushegian, V.V. Gurevich, G protein-coupled receptor kinases: more than just kinases and not only for GPCRs, Pharmacology & therapeutics, 133 (2012) 40-69.

[2] L. Garcia-Guerra, I. Nieto-Vazquez, R. Vila-Bedmar, M. Jurado-Pueyo, G. Zalba, J. Diez, C. Murga, S. Fernandez-Veledo, F. Mayor, Jr., M. Lorenzo, G protein-coupled receptor kinase 2 plays a relevant role in insulin resistance and obesity, Diabetes, 59 (2010) 2407-2417.

[3] R. Vila-Bedmar, L. Garcia-Guerra, I. Nieto-Vazquez, F. Mayor, Jr., M. Lorenzo, C. Murga, S. Fernandez-Veledo, GRK2 contribution to the regulation of energy expenditure and brown fat function, FASEB journal : official publication of the Federation of American Societies for Experimental Biology, 26 (2012) 3503-3514.

[4] M.S. Avendano, E. Lucas, M. Jurado-Pueyo, S. Martinez-Revelles, R. Vila-Bedmar, F. Mayor, Jr., M. Salaices, A.M. Briones, C. Murga, Increased nitric oxide bioavailability in adult GRK2 hemizygous mice protects against angiotensin II-induced hypertension, Hypertension, 63 (2014) 369-375.

[5] P. Penela, C. Murga, C. Ribas, A.S. Tutor, S. Peregrin, F. Mayor, Jr., Mechanisms of regulation of G protein-coupled receptor kinases (GRKs) and cardiovascular disease, Cardiovasc Res, 69 (2006) 46-56.

[6] H. Brinks, A. Das, W.J. Koch, A role for GRK2 in myocardial ischemic injury: indicators of a potential future therapy and diagnostic, Future cardiology, 7 (2011) 547-556.

[7] G.W. Dorn, 2nd, GRK mythology: G-protein receptor kinases in cardiovascular disease, J Mol Med, 87 (2009) 455-463.

[8] P. Penela, C. Murga, C. Ribas, V. Lafarga, F. Mayor Jr., The complex G protein-coupled receptor kinase 2 (GRK2) interactome unveils new physio-pathological targets, British Journal of Pharmacology 160 (2010) 821-832.

[9] H.A. Rockman, D.J. Choi, S.A. Akhter, M. Jaber, B. Giros, R.J. Lefkowitz, M.G. Caron, W.J. Koch, Control of myocardial contractile function by the level of beta-adrenergic receptor kinase 1 in gene-targeted mice, J Biol Chem, 273 (1998) 18180-18184.

[10] C. Ribas, P. Penela, C. Murga, A. Salcedo, C. Garcia-Hoz, M. Jurado-Pueyo, I. Aymerich, F. Mayor, Jr., The G protein-coupled receptor kinase (GRK) interactome: role of GRKs in GPCR regulation and signaling, Biochim Biophys Acta, 1768 (2007) 913-922.

[11] M. Ciccarelli, J.K. Chuprun, G. Rengo, E. Gao, Z. Wei, R.J. Peroutka, J.I. Gold, A. Gumpert, M. Chen, N.J. Otis, G.W. Dorn, 2nd, B. Trimarco, G. Iaccarino, W.J. Koch, G protein-coupled receptor kinase 2 activity impairs cardiac glucose uptake and promotes insulin resistance after myocardial ischemia, Circulation, 123 (2011) 1953-1962.

[12] K. Rett, M. Wicklmayr, G.J. Dietze, H.U. Haring, Insulin-induced glucose transporter (GLUT1 and GLUT4) translocation in cardiac muscle tissue is mimicked by bradykinin, Diabetes, 45 Suppl 1 (1996) S66-69.

[13] D.J. Burks, J. Wang, H. Towery, O. Ishibashi, D. Lowe, H. Riedel, M.F. White, IRS pleckstrin homology domains bind to acidic motifs in proteins, J Biol Chem, 273 (1998) 31061-31067.

[14] A. Cruz-Adalia, L.J. Jimenez-Borreguero, M. Ramirez-Huesca, I. Chico-Calero, O. Barreiro, E. Lopez-Conesa, M. Fresno, F. Sanchez-Madrid, P. Martin, CD69 limits the severity of cardiomyopathy after autoimmune myocarditis, Circulation, 122 (2010) 1396-1404.

[15] M.L. Soto-Montenegro, J.J. Vaquero, J. Pascau, J.D. Gispert, P. Garcia-Barreno, M. Desco, Detection of visual activation in the rat brain using 2-deoxy-2-[(18)F]fluoro-D: -glucose and statistical parametric mapping (SPM), Molecular imaging and biology : MIB : the official publication of the Academy of Molecular Imaging, 11 (2009) 94-99.

[16] L. Bertrand, S. Horman, C. Beauloye, J.L. Vanoverschelde, Insulin signalling in the heart, Cardiovasc Res, 79 (2008) 238-248.

[17] J.G. Miquet, Growth hormone modulation of insulin signaling in the heart, Cell Cycle, 11 (2012) 827-828.

[18] N. Tsybouleva, L. Zhang, S. Chen, R. Patel, S. Lutucuta, S. Nemoto, G. DeFreitas, M. Entman, B.A. Carabello, R. Roberts, A.J. Marian, Aldosterone, through novel signaling proteins, is a fundamental molecular bridge between the genetic defect and the cardiac phenotype of hypertrophic cardiomyopathy, Circulation, 109 (2004) 1284-1291.

[19] A.C. Houweling, M.M. van Borren, A.F. Moorman, V.M. Christoffels, Expression and regulation of the atrial natriuretic factor encoding gene Nppa during development and disease, Cardiovascular research, 67 (2005) 583-593.

[20] N. Sainz, A. Rodriguez, V. Catalan, S. Becerril, B. Ramirez, J. Gomez-Ambrosi, G. Fruhbeck, Leptin administration downregulates the increased expression levels of genes related to oxidative stress and inflammation in the skeletal muscle of ob/ob mice, Mediators of inflammation, 2010 (2010) 784343.

[21] S.J. Matkovich, D.J. Van Booven, A. Hindes, M.Y. Kang, T.E. Druley, F.L. Vallania, R.D. Mitra, M.P. Reilly, T.P. Cappola, G.W. Dorn, 2nd, Cardiac signaling genes exhibit unexpected sequence diversity in sporadic cardiomyopathy, revealing HSPB7 polymorphisms associated with disease, The Journal of clinical investigation, 120 (2010) 280-289.

[22] T. Senbonmatsu, T. Saito, E.J. Landon, O. Watanabe, E. Price, Jr., R.L. Roberts, H. Imboden, T.G. Fitzgerald, F.A. Gaffney, T. Inagami, A novel angiotensin II type 2 receptor signaling pathway: possible role in cardiac hypertrophy, The EMBO journal, 22 (2003) 6471-6482.

[23] A.R. Albig, D.J. Becenti, T.G. Roy, W.P. Schiemann, Microfibril-associate glycoprotein-2 (MAGP-2) promotes angiogenic cell sprouting by blocking notch signaling in endothelial cells, Microvascular research, 76 (2008) 7-14.
[24] R.A. Weir, S. Clements, T. Steedman, H.J. Dargie, J.J. McMurray, I.B. Squire, L.L. Ng, Plasma TIMP-4 predicts left ventricular remodeling after acute myocardial infarction, Journal of cardiac failure, 17 (2011) 465-471.
[25] Y. Eguchi, N. Eguchi, H. Oda, K. Seiki, Y. Kijima, Y. Matsu-ura, Y. Urade, O. Hayaishi, Expression of lipocalin-type prostaglandin D synthase (beta-trace) in human heart and its accumulation in the coronary circulation of angina patients, Proceedings of the National Academy of Sciences of the United States of America, 94 (1997) 14689-14694.
[26] L. Ragolia, T. Palaia, C.E. Hall, J.K. Maesaka, N. Eguchi, Y. Urade, Accelerated glucose intolerance, nephropathy, and atherosclerosis in prostaglandin D2 synthase knock-out mice, The Journal of biological chemistry, 280 (2005) 29946-29955.
[27] J. Lee, Y. Xu, L. Lu, B. Bergman, J.W. Leitner, C. Greyson, B. Draznin, G.G. Schwartz, Multiple abnormalities of myocardial insulin signaling in a porcine model of diet-induced obesity, American journal of physiology. Heart and circulatory physiology, 298 (2010) H310-319.
[28] Y. Terauchi, Y. Tsuji, S. Satoh, H. Minoura, K. Murakami, A. Okuno, K. Inukai, T. Asano, Y. Kaburagi, K. Ueki, H. Nakajima, T. Hanafusa, Y. Matsuzawa, H. Sekihara, Y. Yin, J.C. Barrett, H. Oda, T. Ishikawa, Y. Akanuma, I. Komuro, M. Suzuki, K. Yamamura, T. Kodama, H. Suzuki, S. Koyasu, S. Aizawa, K. Tobe, Y. Fukui, Y. Yazaki, T. Kadowaki, Increased insulin sensitivity and hypoglycaemia in mice lacking the p85 alpha subunit of phosphoinositide 3-kinase, Nature genetics, 21 (1999) 230-235.
[29] C.M. Taniguchi, J.O. Aleman, K. Ueki, J. Luo, T. Asano, H. Kaneto, G. Stephanopoulos, L.C. Cantley, C.R. Kahn, The p85alpha regulatory subunit of phosphoinositide 3-kinase potentiates c-Jun N-terminal kinase-mediated insulin resistance, Molecular and cellular biology, 27 (2007) 2830-2840.
[30] G. Haemmerle, T. Moustafa, G. Woelkart, S. Buttner, A. Schmidt, T. van de Weijer, M. Hesselink, D. Jaeger, P.C. Kienesberger, K. Zierler, R. Schreiber, T. Eichmann, D. Kolb, P. Kotzbeck, M. Schweiger, M. Kumari, S. Eder, G. Schoiswohl, N. Wongsiriroj, N.M. Pollak, F.P. Radner, K. Preiss-Landl, T. Kolbe, T. Rulicke, B. Pieske, M. Trauner, A. Lass, R. Zimmermann, G. Hoefler, S. Cinti, E.E. Kershaw, P. Schrauwen, F. Madeo, B. Mayer, R. Zechner, ATGL-mediated fat catabolism regulates cardiac mitochondrial function via PPAR-alpha and PGC-1, Nat Med, 17 (2011) 1076-1085.
[31] C. Riehle, A.R. Wende, V.G. Zaha, K.M. Pires, B. Wayment, C. Olsen, H. Bugger, J. Buchanan, X. Wang, A.B. Moreira, T. Doenst, G. Medina-Gomez, S.E. Litwin, C.J. Lelliott, A. Vidal-Puig, E.D. Abel, PGC-1beta deficiency accelerates the transition to heart failure in pressure overload hypertrophy, Circ Res, 109 (2011) 783-793.
[32] C.L. Zhang, T.A. McKinsey, S. Chang, C.L. Antos, J.A. Hill, E.N. Olson, Class II histone deacetylases act as signal-responsive repressors of cardiac hypertrophy, Cell, 110 (2002) 479-488.
[33] L. Chang, J. Zhang, Y.H. Tseng, C.Q. Xie, J. Ilany, J.C. Bruning, Z. Sun, X. Zhu, T. Cui, K.A. Youker, Q. Yang, S.M. Day, C.R. Kahn, Y.E. Chen, Rad GTPase deficiency leads to cardiac hypertrophy, Circulation, 116 (2007) 2976-2983.
[34] G. Wang, X. Zhu, W. Xie, P. Han, K. Li, Z. Sun, Y. Wang, C. Chen, R. Song, C. Cao, J. Zhang, C. Wu, J. Liu, H. Cheng, Rad as a novel regulator of excitation-contraction coupling and beta-adrenergic signaling in heart, Circ Res, 106 (2010) 317-327.
[35] A. Abi-Gerges, W. Richter, F. Lefebvre, P. Mateo, A. Varin, C. Heymes, J.L. Samuel, C. Lugnier, M. Conti, R. Fischmeister, G. Vandecasteele, Decreased expression and activity of cAMP phosphodiesterases in cardiac hypertrophy and its impact on beta-adrenergic cAMP signals, Circ Res, 105 (2009) 784-792.
[36] Y. Xia, M. Dobaczewski, C. Gonzalez-Quesada, W. Chen, A. Biernacka, N. Li, D.W. Lee, N.G. Frangogiannis, Endogenous thrombospondin 1 protects the pressure-overloaded myocardium by modulating fibroblast phenotype and matrix metabolism, Hypertension, 58 (2011) 902-911.
[37] W.H. Wu, C.P. Hu, X.P. Chen, W.F. Zhang, X.W. Li, X.M. Xiong, Y.J. Li, MicroRNA-130a mediates proliferation of vascular smooth muscle cells in hypertension, Am J Hypertens, 24 (2011) 1087-1093.
[38] M.L. Simonsen, H.M. Alessio, P. White, D.L. Newsom, A.E. Hagerman, Acute physical activity effects on cardiac gene expression, Exp Physiol, 95 (2010) 1071-1080.
[39] P. Bostrom, N. Mann, J. Wu, P.A. Quintero, E.R. Plovie, D. Panakova, R.K. Gupta, C. Xiao, C.A. MacRae, A. Rosenzweig, B.M. Spiegelman, C/EBPbeta controls exercise-induced cardiac growth and protects against pathological cardiac remodeling, Cell, 143 (2010) 1072-1083.

[40] J.D. Molkentin, The transcription factor C/EBPbeta serves as a master regulator of physiologic cardiac hypertrophy, Circ Res, 108 (2011) 277-278.
[41] C. Sloan, J. Tuinei, K. Nemetz, J. Frandsen, J. Soto, N. Wride, T. Sempokuya, L. Alegria, H. Bugger, E.D. Abel, Central leptin signaling is required to normalize myocardial fatty acid oxidation rates in caloric-restricted ob/ob mice, Diabetes, 60 (2011) 1424-1434.
[42] H. Zhang, C.A. Makarewich, H. Kubo, W. Wang, J.M. Duran, Y. Li, R.M. Berretta, W.J. Koch, X. Chen, E. Gao, H.H. Valdivia, S.R. Houser, Hyperphosphorylation of the cardiac ryanodine receptor at serine 2808 is not involved in cardiac dysfunction after myocardial infarction, Circulation research, 110 (2012) 831-840.
[43] H. Bugger, E.D. Abel, Rodent models of diabetic cardiomyopathy, Dis Model Mech, 2 (2009) 454-466.
[44] S. Boudina, H. Bugger, S. Sena, B.T. O'Neill, V.G. Zaha, O. Ilkun, J.J. Wright, P.K. Mazumder, E. Palfreyman, T.J. Tidwell, H. Theobald, O. Khalimonchuk, B. Wayment, X. Sheng, K.J. Rodnick, R. Centini, D. Chen, S.E. Litwin, B.E. Weimer, E.D. Abel, Contribution of impaired myocardial insulin signaling to mitochondrial dysfunction and oxidative stress in the heart, Circulation, 119 (2009) 1272-1283.
[45] D.D. Belke, S. Betuing, M.J. Tuttle, C. Graveleau, M.E. Young, M. Pham, D. Zhang, R.C. Cooksey, D.A. McClain, S.E. Litwin, H. Taegtmeyer, D. Severson, C.R. Kahn, E.D. Abel, Insulin signaling coordinately regulates cardiac size, metabolism, and contractile protein isoform expression, J Clin Invest, 109 (2002) 629-639.
[46] R. Aikawa, M. Nawano, Y. Gu, H. Katagiri, T. Asano, W. Zhu, R. Nagai, I. Komuro, Insulin prevents cardiomyocytes from oxidative stress-induced apoptosis through activation of PI3 kinase/Akt, Circulation, 102 (2000) 2873-2879.
[47] H. Ashrafian, M.P. Frenneaux, L.H. Opie, Metabolic mechanisms in heart failure, Circulation, 116 (2007) 434-448.
[48] I. Shimizu, Y. Yoshida, T. Katsuno, K. Tateno, S. Okada, J. Moriya, M. Yokoyama, A. Nojima, T. Ito, R. Zechner, I. Komuro, Y. Kobayashi, T. Minamino, p53-induced adipose tissue inflammation is critically involved in the development of insulin resistance in heart failure, Cell Metab, 15 (2012) 51-64.
[49] L.H. Opie, The metabolic vicious cycle in heart failure, Lancet, 364 (2004) 1733-1734.
[50] H. von Bibra, M. St John Sutton, Impact of diabetes on postinfarction heart failure and left ventricular remodeling, Curr Heart Fail Rep, 8 (2011) 242-251.
[51] J.A. Hata, M.L. Williams, J.N. Schroder, B. Lima, J.R. Keys, B.C. Blaxall, J.A. Petrofski, A. Jakoi, C.A. Milano, W.J. Koch, Lymphocyte levels of GRK2 (betaARK1) mirror changes in the LVAD-supported failing human heart: lower GRK2 associated with improved beta-adrenergic signaling after mechanical unloading, J Card Fail, 12 (2006) 360-368.
[52] A. Chokshi, K. Drosatos, F.H. Cheema, R. Ji, T. Khawaja, S. Yu, T. Kato, R. Khan, H. Takayama, R. Knoll, H. Milting, C.S. Chung, U. Jorde, Y. Naka, D.M. Mancini, I.J. Goldberg, P.C. Schulze, Ventricular assist device implantation corrects myocardial lipotoxicity, reverses insulin resistance, and normalizes cardiac metabolism in patients with advanced heart failure, Circulation, 125 (2012) 2844-2853.
[53] G. Rengo, G. Galasso, G.D. Femminella, V. Parisi, C. Zincarelli, G. Pagano, C. De Lucia, A. Cannavo, D. Liccardo, C. Marciano, C. Vigorito, F. Giallauria, N. Ferrara, G. Furgi, P. Perrone Filardi, W.J. Koch, D. Leosco, Reduction of lymphocyte G protein-coupled receptor kinase-2 (GRK2) after exercise training predicts survival in patients with heart failure, Eur J Prev Cardiol, (2013).

529

530

531

532

533

534

535

Figure 1 **Lucas and Jurado-Pueyo et al**

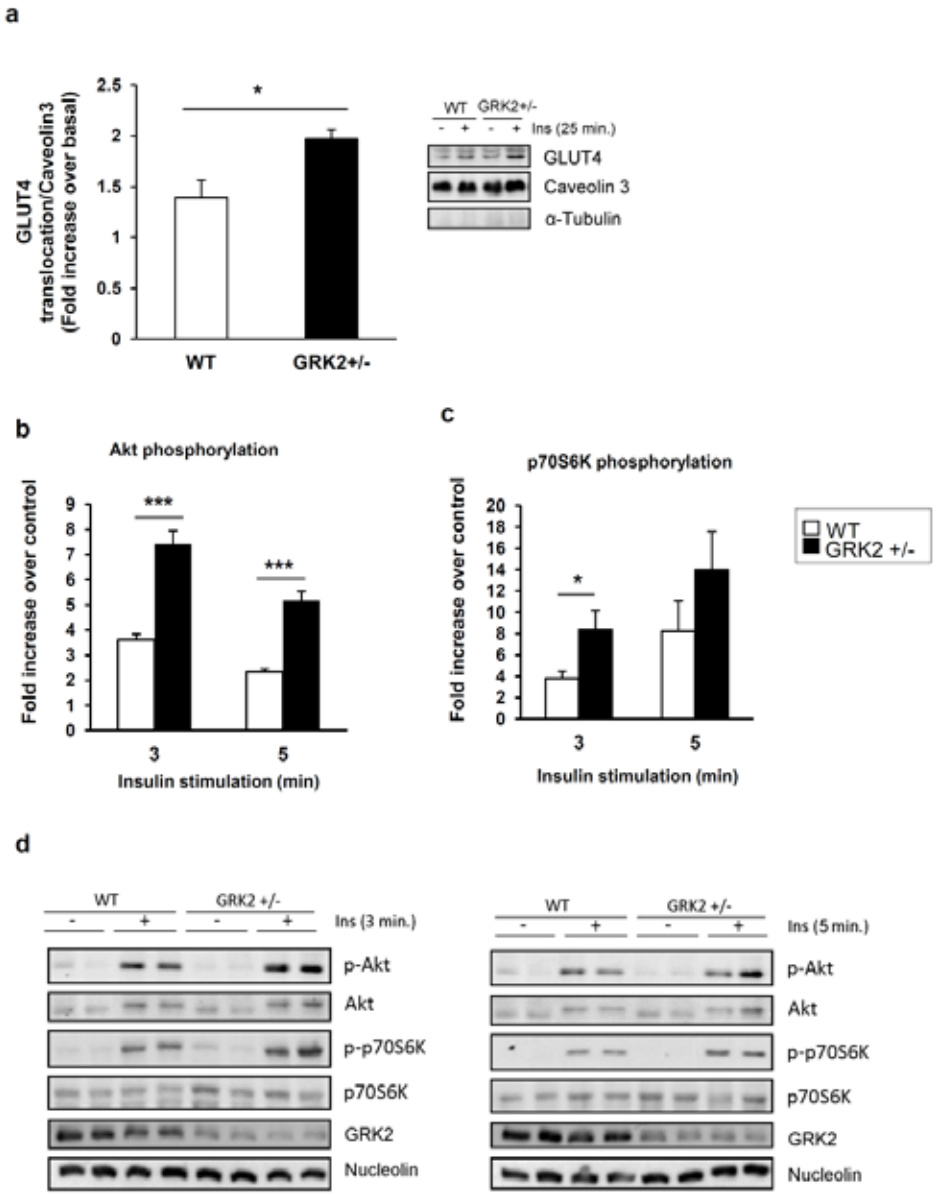

Figure 1. GLUT4 translocation to the membrane and insulin signalling are upregulated in hearts from adult GRK2$^{+/-}$ mice. a). GLUT4 translocation in the plasma membrane fraction after an intravenous injection of insulin for 25 minutes in 9 month-old WT and GRK2+/- mice (N=6-8 per genotype). Results were normalized to Caveolin 3 levels and are expressed as fold increase over basal (non-insulin treated mice). Representative blots are shown including α-Tubulin blot as an indicator of the absence of cytosolic contamination. Quantification of Akt phosphorylation (Ser473) (**b)** and p70S6K phosphorylation (Thr389) (**c**) in the cardiac tissue lysates of WT or GRK2$^{+/-}$ 9 month-old mice after an intravenous injection of insulin for 3 or 5 minutes (N=3-5). Results are expressed as fold increase over control (non-insulin treated mice). **d)** Representative Western Blots of the specified phospho-proteins and controls in heart tissue 3 or 5 min after insulin injection. Data are mean±SEM of the indicated independent experiments. ***,p<0.001; *,p<0.05

Figure 2 **Lucas and Jurado-Pueyo et al**

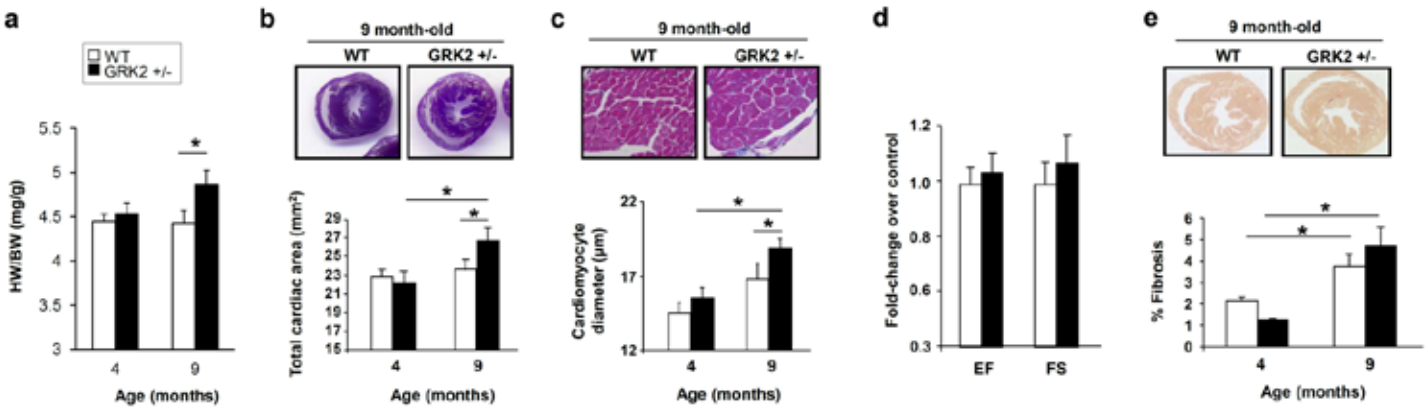

Figure 2. GRK2$^{+/-}$ 9 month-old mice show mild, non-pathological heart hypertrophy. a) Heart weight (mg) to body weight (g) ratio in 4 and 9 month-old WT and GRK2$^{+/-}$ mice (N=7-14). **b)** Total area of cross sections of each heart was measured from high-resolution images using the AnalySIS® software and expressed in mm^2 for WT (white bars) and GRK2$^{+/-}$ (black bars) mice (N=5-9). **c)** Cardiomyocyte diameter (in µm) was measured in the cross-section of cells perpendicular to the slices stained with Masson´s Trichrome in at least 20 cells per sample using the AnalySIS® software (N=5-9). **d)** Fold change of ejection fraction (EF) and fractional shortening (FS), with statistical analysis performed using T- test. **e)** Quantification of the fibrotic area of heart cross sections stained with Syrius Red, digitalized using the Axiovision software and analyzed using the AnalySIS® software. Representative pictures are shown when applicable. Data are mean±SEM of the indicated independent experiments *, $p<0.05$

a

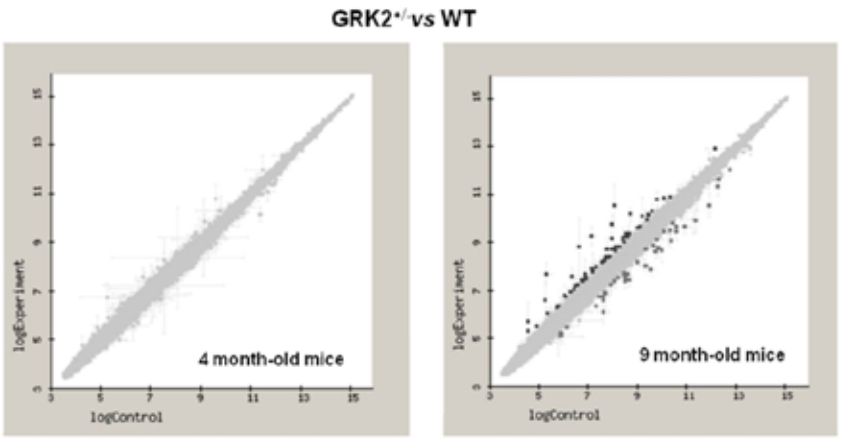

b

Genes	GRK2 +/- vs WT	Pathological heart hypertrophy Diabetes/Obesity
Rrad *Thbs1* *Pde4b* *Hdac9* *Nr4a1* *Tcf7L2* *Slc2a3* *Aqp7* *Meox2* *Ppargc1b*	Upregulated	Downregulated
Zbtb16 *Timp4* *Ptgds* *Acta1* *Nppa* *Hspb7* *Mfap5* *Pi3kr1*	Downregulated	Upregulated

Genes	GRK2 +/- vs WT	Physiological heart hypertrophy Response to exercise
Ppargc1b *Nr4a1* *Fosb* *Apold1*	Upregulated	Upregulated
Cebpb	Downregulated	Downregulated

Figure 3. Comparison of cardiac gene expression profiles between young (4 month-old) or adult (9 month-old) WT and GRK2$^{+/-}$ mice. a) Genes whose expression varied significantly between WT and GRK2$^{+/-}$ mice are represented. Pairwise analyses were performed and visualized using the FIESTA viewer for an FDR<0.2 (Fold change >1.5 or <-1.5). No genes were found to change significantly at 4 months of age, but, at 9 months of age, 61 genes were significantly different between WT and GRK2$^{+/-}$ mice. Black, genes whose expression is increased in GRK2$^{+/-}$ *vs* WT. Grey, genes whose expression is reduced in GRK2$^{+/-}$ *vs* WT. **b)** The table depicts genes reported to be upregulated during pathological heart hypertrophy or during comorbidities such as diabetes/obesity (see references in the text) found to be downregulated in adult GRK2$^{+/-}$ mice *vs* WT heart microarray, or genes for which the inverse relationship occurs (left panel). Also, a list of genes upregulated/downregulated in the array and also during physiological heart hypertrophy or response to exercise is specified (right panel).

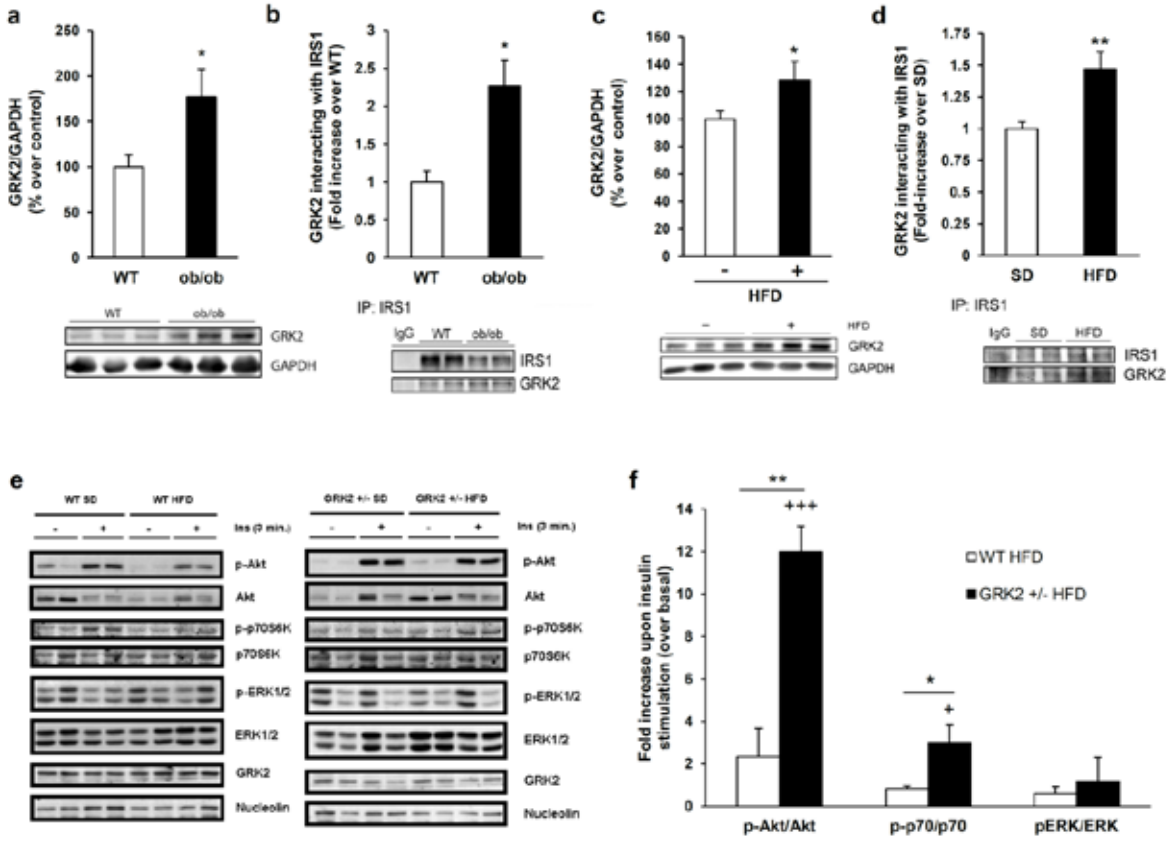

Figure 4. Expression of the GRK2 protein is increased in myocardial tissue of obese or high fat diet-fed mice which correlates with higher levels of IRS1/GRK2 complexes, whereas GRK2$^{+/-}$ animals are resistant to high fat diet-induced insulin resistance in cardiac tissue. a) The expression levels of GRK2 were analyzed by Western Blot in cardiac tissue of 8 month-old ob/ob or WT mice and quantified by densitometry analysis. Results were normalized by GAPDH protein levels and expressed as percent over control (WT mice) (N= 5). **b**) Total protein from heart tissue (500 µg) was immunoprecipitated with the anti-IRS1 or anti-IgG antibodies, and the resulting immune complexes were analyzed by Western blot with the corresponding antibodies against GRK2 and IRS1.(N=3). Precipitated GRK2 amount was normalized with immunoprecipitated IRS1 amount. Same for 3 month-old HFD-fed mice represented over standard diet-fed animals in (**c**) and (**d**) (N= 9). Representative blots are shown. Data are mean±SEM of the indicated independent experiments *,p<0.05; **,p<0.01. **e)** Representative Western Blots of the specified phospho-proteins and controls in heart tissue after 12 weeks of HFD feeding or SD and 3 min insulin injection in WT or GRK2$^{+/-}$ mice. (**f)** Quantification of Akt phosphorylation (Ser473), p70S6K phosphorylation (Thr389) or ERK1/2 phosphorylation (Thr202/Tyr204) in cardiac tissue lysates of WT and GRK2+/- mice after 12 weeks of HFD feeding after an intravenous injection of insulin for 3 minutes (N= 3-4). Results are expressed as fold increase over basal (untreated mice). Statistical analysis was performed using T-test. Data are mean±SEM of the indicated independent experiments.+++p<0.001;+p<0.05 referred to basal (untreated mice); **p<0.01; *p<0.05 referred to fold increase upon insulin stimulation over HFD fed WT mice.

Figure 5 **Lucas and Jurado-Pueyo et al**

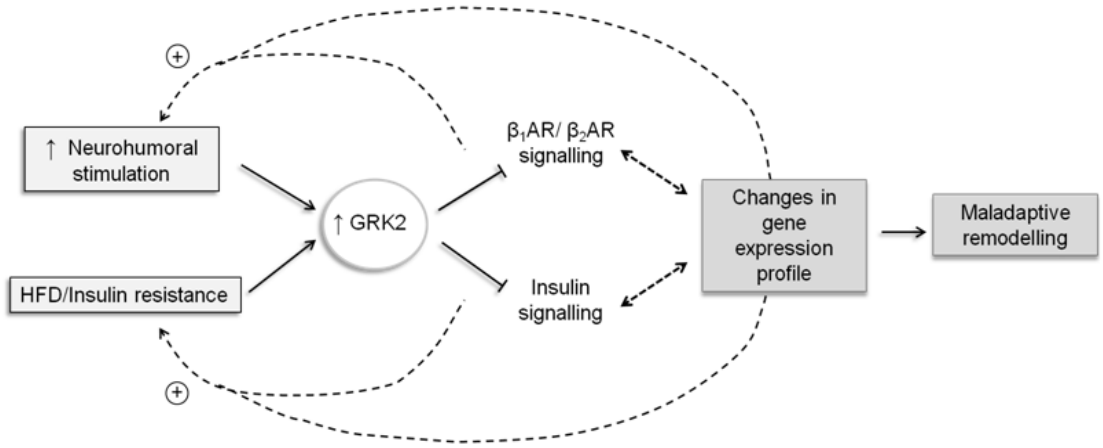

Figure 5. Schematic representation of the proposed model of GRK2 up-regulation linking insulin-resistance and maladaptive cardiac remodeling. Increased GRK2 as a result of different pathophysiological situations would not only lead to a decrease in β-AR responsiveness, but also in insulin signaling thus promoting a pathological increase in the neurohumoral stimulation of the heart, and also lead to IR thus aggravating this condition. GRK2-promoted transcription reprogramming would also impinge upon both processes.

SUPPLEMENTAL TABLES AND FIGURES

Supplemental Table 1S. Detailed list of genes showing differential expression between WT and GRK2$^{+/-}$ adult hearts.

Genes whose expression varied with an FDR<0.2 and a Fold change >1.5 or <-1.5 are listed.

9 month-old +/- vs. 9 month-old wt

Fold-change	p-val (LiMMA)	Probe ID	Gene symbol/Gene title
+5.68	0.00087794	1417065_at	Egr1 | early growth response 1
+5.40	0.00001080	1436329_at	Egr3 | early growth response 3
+4.49	0.00001003	1448756_at	S100a9 | S100 calcium binding protein A9 (calgranulin B)
+3.59	0.00002794	1419394_s_at	S100a8 | S100 calcium binding protein A8 (calgranulin A)
+2.81	0.00002836	1416505_at	Nr4a1 | nuclear receptor subfamily 4, group A, member 1
+1.78	0.00031535	1435207_at	Dixdc1 | DIX domain containing 1
+1.73	0.00010339	1426952_at	Arhgap18 | Rho GTPase activating protein 18
+1.73	0.00000815	1449945_at	Ppargc1b | peroxisome proliferative activated receptor, gamma, coactivator 1 beta
+1.70	0.00097468	1421811_at	Thbs1 | thrombospondin 1 /// similar to thrombospondin 1
+1.69	0.00112735	1450407_a_at	Anp32a | acidic (leucine-rich) nuclear phosphoprotein 32 family, member A
+1.66	0.00011584	1424234_s_at	Meox2 | mesenchyme homeobox 2
+1.66	0.00076817	1457644_s_at	Cxcl1 | chemokine (C-X-C motif) ligand 1
+1.64	0.00189368	1419156_at	Sox4 | SRY-box containing gene 4 /// similar to Transcription factor SOX-4
+1.64	0.00029988	1447457_at	Ada | Adenosine deaminase
+1.61	0.00039396	1418849_x_at	Aqp7 | aquaporin 7
+1.59	0.00035215	1436600_at	Tnrc9 | trinucleotide repeat containing 9
+1.58	0.00023340	1437052_s_at	Slc2a3 | solute carrier family 2 (facilitated glucose transporter), member 3
+1.58	0.00026865	1439766_x_at	Vegfc | vascular endothelial growth factor C
+1.58	0.00242113	1456735_x_at	Acpl2 | acid phosphatase-like 2
+1.57	0.00001115	1433651_at	Wtip | WT1-interacting protein
+1.56	0.00005950	1457432_at	Prox1 | prospero-related homeobox 1
+1.55	0.00088244	1422134_at	Fosb | FBJ osteosarcoma oncogene B
+1.55	0.00001032	1422474_at	Pde4b | phosphodiesterase 4B, cAMP specific
+1.54	0.00181760	1434856_at	Ankrd44 | ankyrin repeat domain 44
+1.53	0.00129704	1448382_at	Ehhadh | enoyl-Coenzyme A, hydratase/3-hydroxyacyl Coenzyme A dehydrogenase
+1.53	0.00020216	1457139_at	Auts2 | autism susceptibility candidate 2
+1.52	0.00007822	1422562_at	Rrad | Ras-related associated with diabetes
+1.52	0.00203143	1423489_at	Mmd | monocyte to macrophage differentiation-associated
+1.52	0.00034652	1441228_at	Apold1 | apolipoprotein L domain containing 1
+1.52	0.00018939	1444952_a_at	Nucks1 | nuclear casein kinase and cyclin-dependent kinase substrate 1
+1.51	0.00011940	1429427_s_at	Tcf7l2 | transcription factor 7-like 2, T-cell specific, HMG-box
+1.51	0.00050197	1434572_at	Hdac9 | histone deacetylase 9
+1.51	0.00168651	1456005_a_at	Bcl2l11 | BCL2-like 11 (apoptosis facilitator)

Fold-change	p-val (LiMMA)	Probe ID	Gene symbol/Gene title
-1.51	0.00052884	1423233_at	Cebpd | CCAAT/enhancer binding protein (C/EBP), delta
-1.51	0.00128321	1425281_a_at	Tsc22d3 | TSC22 domain family 3
-1.53	0.00079516	1419598_at	Ms4a6d | membrane-spanning 4-domains, subfamily A, member 6D
-1.53	0.00190063	1435459_at	Fmo2 | flavin containing monooxygenase 2
-1.54	0.00052036	1448185_at	Herpud1 | homocysteine-inducible, endoplasmic reticulum stress-inducible, ubiquitin-like domain member 1
-1.54	0.00016858	1449082_at	Mfap5 | microfibrillar associated protein 5
-1.56	0.00029120	1428547_at	Nt5e | 5 nucleotidase, ecto
-1.57	0.00216211	1421289_at	Hspb7 | heat shock protein family, member 7 (cardiovascular)
-1.58	0.00169451	1425515_at	Pik3r1 | phosphatidylinositol 3-kinase, regulatory subunit, polypeptide 1 (p85 alpha)
-1.58	0.00088349	1455399_at	Cnksr1 | connector enhancer of kinase suppressor of Ras 1 /// similar to connector enhancer of kinase suppressor of Ras1
-1.60	0.00025712	1454638_a_at	Pah | phenylalanine hydroxylase
-1.67	0.00001101	1428776_at	Slc10a6 | solute carrier family 10 (sodium/bile acid cotransporter family), member 6
-1.68	0.00055243	1438009_at	MGC73635 | similar to histone 2a
-1.72	0.00063349	1434437_x_at	Rrm2 | ribonucleotide reductase M2
-1.72	0.00004522	1439153_at	Ibrdc2 | IBR domain containing 2
-1.73	0.00011780	1427844_a_at	Cebpb | CCAAT/enhancer binding protein (C/EBP), beta
-1.78	0.00214243	1425645_s_at	Cyp2b10 | cytochrome P450, family 2, subfamily b, polypeptide 10
-1.81	0.00008762	1427638_at	Zbtb16 | zinc finger and BTB domain containing 16
-1.85	0.00010205	1427345_a_at	Sult1a1 | sulfotransferase family 1A, phenol-preferring, member 1
-1.89	0.00012300	1425303_at	Gck | glucokinase
-1.90	0.00256270	1423860_at	Ptgds | prostaglandin D2 synthase (brain)
-1.94	0.00108646	1428352_at	Arrdc2 | arrestin domain containing 2
-2.16	0.00058602	1450974_at	Timp4 | tissue inhibitor of metalloproteinase 4
-2.32	0.00063394	1456062_at	Nppa | natriuretic peptide precursor type A
-2.39	0.00002699	1416125_at	Fkbp5 | FK506 binding protein 5
-2.43	0.00002224	1416225_at	Adh1 | alcohol dehydrogenase 1 (class I)
-2.47	0.00164694	1427735_a_at	Acta1 | actin, alpha 1, skeletal muscle
-2.76	0.00070986	1417600_at	Slc15a2 | solute carrier family 15 (H+/peptide transporter), member 2

Supplemental Figure 1S

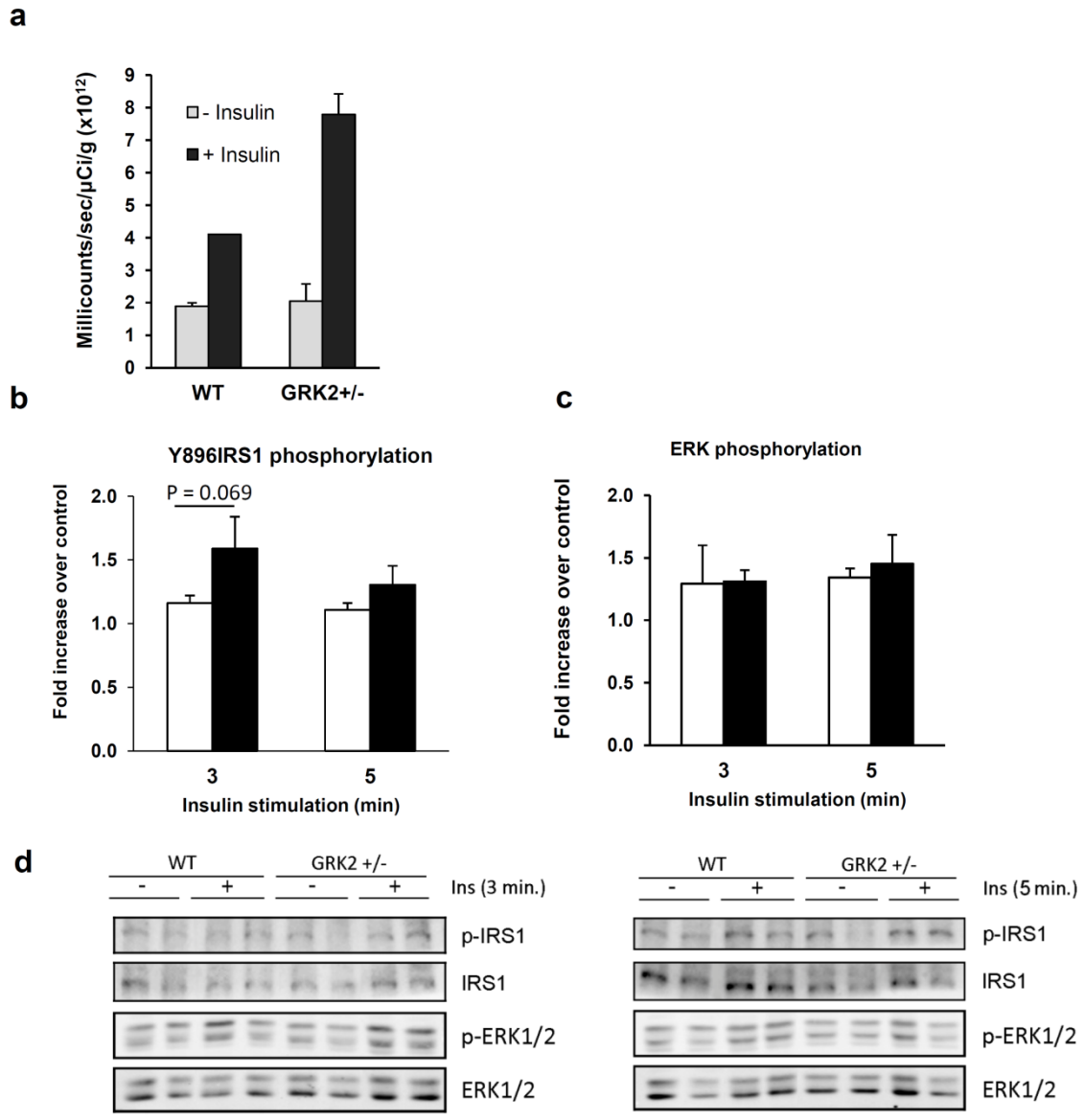

Suppl. Fig.1S.- Glucose uptake and insulin signalling are upregulated in hearts from adult GRK2+/- mice without differences in pERK activation. a) Positron emission tomography (PET) analysis of insulin-dependent 18F-Fluoro deoxy-glucose uptake in the hearts of 9 month-old WT and GRK2+/- mice (N=3 per genotype). Quantification of IRS1 phosphorylation (Tyr896) (b) and ERK1/2 phosphorylation (Thr202/Tyr204) (c) in the cardiac tissue lysates of WT or GRK2+/- 9 month-old mice after an intravenous injection of insulin for 3 or 5 minutes (N=3-5). Results are expressed as fold increase over control (non-insulin treated mice). d) Representative Western Blots of the specified phospho-proteins and controls in heart tissue 3 or 5 min after insulin injection. Data are mean±SEM of the indicated independent experiments.

Supplemental Figure 2S

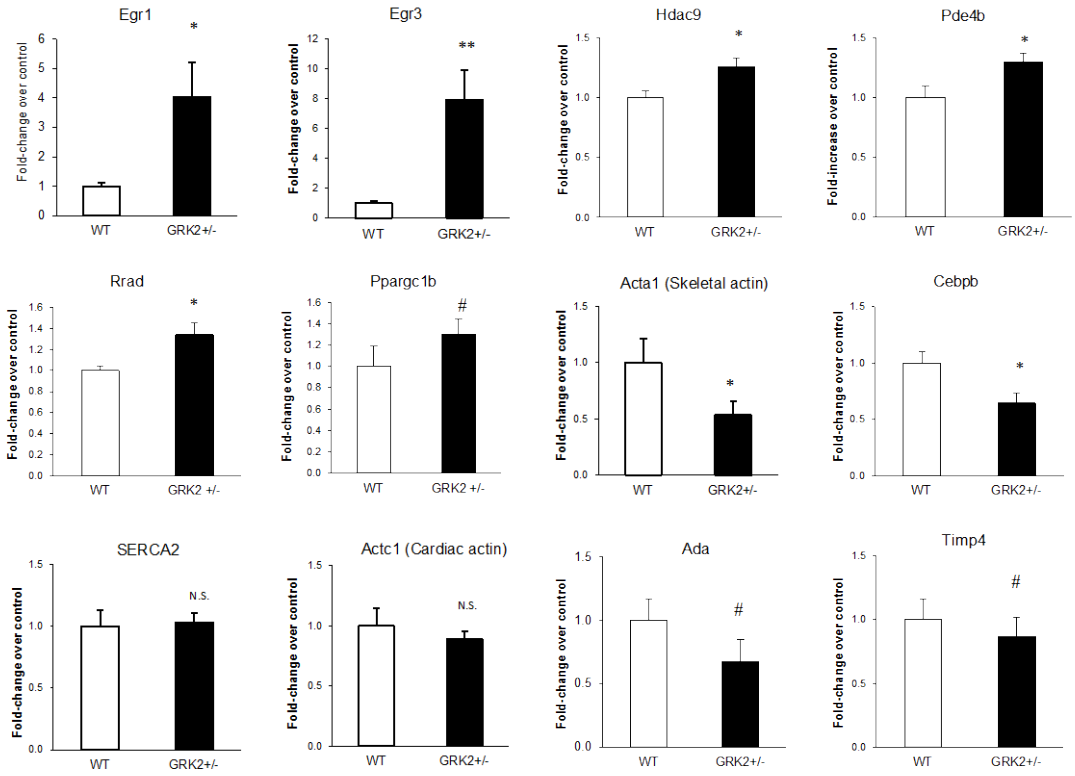

Suppl. Fig.2S.- Validation by qRT-PCR analysis**.** A qRT-PCR analysis was performed for certain genes whose changes in expression are described to correlate with physiological or pathological cardiac hypertrophy or other cardiac responses important for cardiac physiopathology as discussed in the main text. * $p<0.05$, # $0.2>p>0.05$.